J|A|C|S COMMUNICATIONS

Published on Web 05/04/2009

Polymerization of Phenylacetylene by Rhodium Complexes within a Discrete Space of apo-Ferritin

Satoshi Abe,[†] Kunio Hirata,[‡,§] Takafumi Ueno,*[,†,⊥] Kazuhide Morino,[||] Nobutaka Shimizu,[§] Masaki Yamamoto,[‡,§] Masaki Takata,[‡,§,#] Eiji Yashima,[||] and Yoshihito Watanabe*[,¶]

Institute for Integrated Cell-Material Sciences (iCeMS), Funai Center, Kyoto University, Katsura, Nishikyo-ku, Kyoto 615-8510, Japan, RIKEN SPring-8 Center, Sayo-gun, Hyogo 679-5198, Japan, Japan Synchrotron Radiation Research Institute, Sayo-gun, Hyogo 679-5198, Japan, PRESTO, Japan Science and Technology Agency (JST), Saitama 332-0012, Japan, Department of Molecular Design and Engineering, Graduate School of Engineering, Nagoya University, Nagoya 464-8603, Japan, The University of Tokyo and CREST, JST and Research Center for Materials Science, Nagoya University, Nagoya 464-8602, Japan

Received February 17, 2009; E-mail: taka@sbchem.kyoto-u.ac.jp; yoshi@nucc.cc.nagoya-u.ac.jp

Self-assembled molecular cages provide powerful platforms for recognition, storage, and catalytic reactions.[1] Many types of molecules, such as proteins,[2−7] polymers,[8,9] and metal complexes,[10−12] have been utilized as components of systems designed to regulate the functions of the cages. Proteins are able to form large spherical cages ranging from several tens to hundreds of nanometers. The protein cages provide the capabilities of preparation and/or storage of nanosized molecular materials such as metal nanoparticles, enzymes, and polymers.[4,13−15] For example, it has been demonstrated that small heat shock protein (sHsp) containing a Pt nanoparticle catalyzes the production of hydrogen gas.[13] When one horseradish peroxidase (HRP) molecule was encapsulated within the cage of Cowpea chlorotic mottle virus (CCMV), the composite maintained the oxidation activity of HRP.[4] These results suggest that protein cages could provide useful reaction spaces through introduction of molecular catalysts into the cages.

Ferritin (Fr), a spherical protein composed of 24 subunits with an 8 nm diameter interior space (Figure 1a,b), is capable of accumulating up to 4500 iron atoms as ferric oxyhydroxides within the cage.[16,17] Metal ions and small organic molecules are able to penetrate the 3-fold axis channels located at the intersections of three subunits of apo-Fr (Figure 1c).[18] apo-Fr has been used to prepare inorganic materials such as quantum dots as well as magnetic and catalytic nanoparticles.[2,14,19−23] More recently, we have demonstrated redox and Suzuki coupling reactions catalyzed by ferrocene and Pd(allyl) complexes, respectively, with these complexes deposited on the interior surface of apo-Fr.[24,25] The crystal structure of the Pd(allyl)·apo-Fr composite shows that the Pd(allyl) complexes form thiol-bridged dinuclear complexes on the interior surface of apo-Fr. These results suggest that apo-Fr is a good candidate for immobilizing synthetic metal complex catalysts and serving as a catalytic reaction space. In this paper, we present polymerization reactions of phenylacetylene and its derivatives catalyzed by Rh(nbd) (nbd = norbornadiene)[26,27] complexes immobilized within the apo-Fr cage. Such polymerization reactions occurring within a discrete space could provide polymers with restricted molecular weight and a narrow molecular weight distribution.

An acetonitrile solution of $[Rh(nbd)Cl]_2$ (1 mL, 10 mM) was treated with a recombinant L-chain apo-Fr from horse liver [10 mL, 10 μM in 50 mM Tris/HCl (pH 8.0), 0.15 M NaCl], and the reaction mixture (9% acetonitrile aqueous solution) was stirred for 1 h at 25 °C. A small amount of acetonitrile was added to increase the solubility of $[Rh(nbd)Cl]_2$ in the reaction medium, as reported previously.[25] After dialysis against a 0.15 M NaCl aqueous solution, the apo-Fr-containing Rh(nbd) complex (**Rh(nbd)·apo-Fr**) was purified with a size-exclusion column (ÄKTA design, Superdex G-200) to remove unbound Rh complexes. The quantity of Rh atoms incorporated into **Rh(nbd)·apo-Fr** was estimated by inductively coupled plasma−optical emission spectrometry (ICP−OES) and bicinchoninate (BCA) analyses. These analyses showed that 57.5 ± 3.5 Rh atoms per apo-Fr were maintained within the cage. When apo-Fr was treated with 200 equiv of $RhCl_3$ instead of $[Rh(nbd)Cl]_2$ (100 equiv) under the same conditions, only 4.8 ± 0.6 Rh atoms remained within apo-Fr. The large difference between $[Rh(nbd)Cl]_2$ and $RhCl_3$ is expected to be due to an extremely slow ligand-exchange rate of $RhCl_3$ with water molecules.[28] $[Rh(nbd)Cl]_2$ complexes are expected to penetrate more smoothly into the cage by the decomposition to mononuclear Rh(nbd) aqua complexes in water.[29]

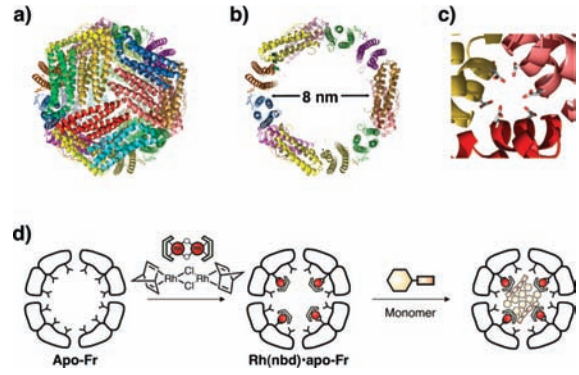

Figure 1. (a−c) Ribbon diagrams of L-ferritin taken from PDB entry 1DAT: (a) the 24-subunit assembled cage; (b) the inner cavity; (c) the 3-fold axis channel. (d) Schematic representation of insertion of $[Rh(nbd)Cl]_2$ into the apo-Fr cage and polymerization catalyzed by the **Rh(nbd)·apo-Fr** composite.

A crystal of **Rh(nbd)·apo-Fr** was obtained by a hanging-drop vapor diffusion method in the presence of cadmium ions, as reported previously.[25,30,31] The crystal structure of **Rh(nbd)·apo-Fr** was refined to 1.80 Å resolution, as shown in Figure 2a. The X-ray data and refinement statistics are summarized in Table S1 in the Supporting Information.[32] The root-mean-square deviation of the C^{α} atoms of **Rh(nbd)·apo-Fr** from that of apo-Fr (0.42 Å) indicates

[†] iCeMS, Kyoto University.
[‡] RIKEN SPrng-8 Center.
[§] Japan Synchrotron Radiation Research Institute.
[⊥] PRESTO, Japan Science and Technology Agency (JST).
[||] Department of Molecular Design and Engineering, Nagoya University.
[#] The University of Tokyo and CREST, JST.
[¶] Research Center for Materials Science, Nagoya University.

10.1021/ja901234j CCC: $40.75

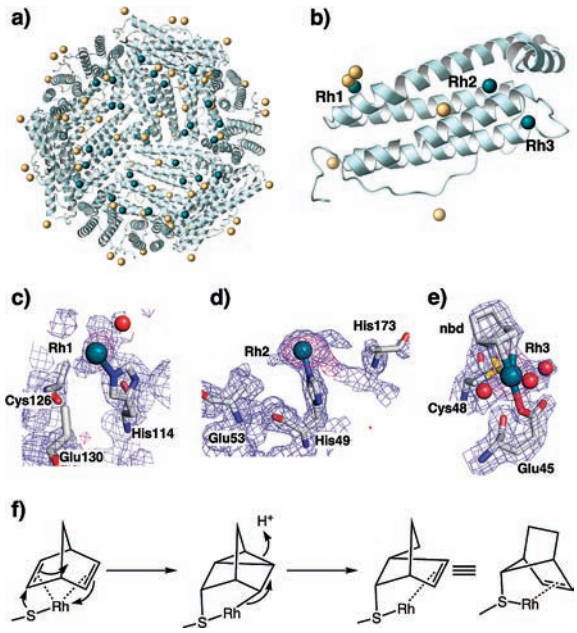

Figure 2. (a−e) Crystal structures of **Rh(nbd)·apo-Fr**: (a) the whole structure; (b) a subunit structure containing Rh atoms (greenish-blue spheres) and Cd atoms (beige spheres); and close views of the coordination structures of (c) the Rh1 binding site at the 3-fold axis channel and (d) the Rh2 and (e) Rh3 sites at the accumulation center. Cys126, Glu130, Glu53, and His173 have been replaced by Ala residues because of the disordered electron densities of the side chains. Anomalous difference Fourier maps at 4.0σ indicate the positions of the Rh atoms as shown in magenta. The $2|F_o| - |F_c|$ electron density maps are colored in blue at 1.0σ. (f) Proposed mechanism of unusual cross-linking of Cys48 with Rh(nbd) of **Rh(nbd)·apo-Fr** at the Rh3 site.

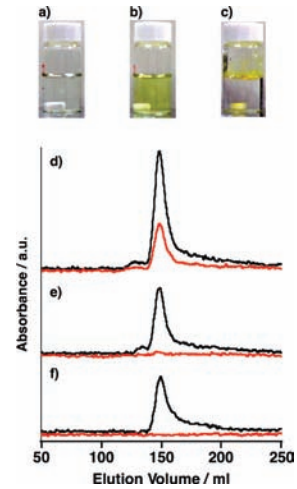

Figure 3. Polymerization of phenylacetylene catalyzed by **Rh(nbd)·apo-Fr**. (a) Solution of **Rh(nbd)·apo-Fr** prior to addition of phenylacetylene (b) Reaction mixture of **Rh(nbd)·apo-Fr** and phenylacetylene after stirring for 3 h at 25 °C. (c) Reaction mixture of $[Rh(nbd)Cl]_2$ and phenylacetylene under the same conditions. (d−f) Elution profiles from size-exclusion chromatography of (d) **Rh(nbd)·apo-Fr** after the reaction, (e) **Rh(nbd)·apo-Fr**, and (f) apo-Fr. Elution was monitored at both 280 nm (black line) and 383 nm (red line).

that the overall structure of **Rh(nbd)·apo-Fr** is quite similar to that of apo-Fr.[30] The anomalous maps indicate that the total numbers of Rh and Cd binding positions per apo-Fr are 72 and 144, respectively (Figure 2a). Each of the three Rh atoms on each ferritin subunit is located on the interior surface of the apo-Fr molecule. One Rh atom (Rh1) is located at the 3-fold axis channel, and the other Rh atoms (Rh2 and Rh3) are bound to the accumulation center (Figure 2a,b). At the 3-fold channel, the Rh1 atom ligates to the N^{ϵ} atom of His114 with a bond distance of 2.13 Å (Figure 2c). At the accumulation center, Rh2 is bound to N^{ϵ} of His49 with a bond distance of 1.93 Å (Figure 2d). Electron density corresponding to the nbd ligand was not observed in the vicinity of Rh1 and Rh2. The side-chain structures of Cys126 and Glu130, which are located near Rh1, and of Glu53 and His173, which are close to Rh2, were also not determined as a result of disorder. On the other hand, the coordination structure of Rh3 is different from the coordination structures of Rh1 and Rh2 because Rh3 is bound not only to O^{ϵ} of Glu45, S^{γ} of Cys48, and three water molecules but also to an nbd ligand, which is in turn bound to S^{γ} of Cys48 (Figure 2e). This cross-link appears to stabilize the coordination of the nbd ligand to the Rh3 atom. The unusual cross-linking of cysteine has also been identified in a cofactor binding site of a quinohemoprotein amine dehydrogenase.[33] The reaction might proceed through an intermediate induced by the coordination of Rh(nbd) (Figure 2f).

The polymerization of phenylacetylene to afford polyphenylacetylene by employing **Rh(nbd)·apo-Fr** was examined as follows: 3000 equiv of phenylacetylene monomer (1.5 mM) was added to a 0.15 M NaCl aqueous solution of **Rh(nbd)·apo-Fr** (0.5 μM) in the presence of NaOH (0.3 mM), and the solution was stirred for 3 h at 25 °C under an argon atmosphere; the color of the reaction mixture subsequently changed from colorless to pale-yellow as a result of the formation of polyphenylacetylene in the apo-Fr cage (Figure 3a,b). This polymerization of phenylacetylene was promoted by Rh(nbd) complexes incorporated in the cage of apo-Fr, because apo-Fr without Rh(nbd) complexes did not catalyze the reaction under the same conditions. On the other hand, the same reaction catalyzed by $[Rh(nbd)Cl]_2$ in the absence of apo-Fr (15 μM $[Rh(nbd)Cl]_2$ in 0.15% acetonitrile aqueous solution) produced water-insoluble polyphenylacetylene (Figure 3c). The reaction solution of **Rh(nbd)·apo-Fr** and phenylacetylene monomer also gave a typical UV−vis absorption spectrum attributed to polyphenylacetylene in the 300−500 nm wavelength range (see the Supporting Information).[34] The size-exclusion column chromatography (ÄKTA design, Superdex G-200) elution profile of the **Rh(nbd)·apo-Fr** after the polymerization showed coelution of protein (280 nm) and polyphenylacetylene (383 nm) components (Figure 3d). In addition, the elution volume of the peak was the same as the elution volumes of **Rh(nbd)·apo-Fr** and apo-Fr (Figure 3e,f). These results indicate that the polymerization of phenylacetylene proceeds in the apo-Fr cage and that the spherical 24-mer assembly of **Rh(nbd)·apo-Fr** maintains its structure during polymerization. To evaluate the stereoregularity and molecular weight of the resulting polymer in **Rh(nbd)·apo-Fr**, the polymer was extracted from the **Rh(nbd)·apo-Fr** cage at pH 2, where the ferritin molecule is dissociated into subunits, allowing easy extraction of the polymer.[35] **Rh(nbd)·apo-Fr** afforded a cis-transoidal main chain of polyphenylacetylene, as confirmed by the ^{1}H NMR signal of the *cis*-olefin proton at 5.84 ppm in $CDCl_3$.[36] This cis-transoidal configuration is identical to the configurations of polyphenylacetylenes produced by catalysis using Rh complexes.[26,37,38] The number-average molecular weights (M_n) of the polyphenylacetylene polymers produced by catalysis using **Rh(nbd)·apo-Fr** and $[Rh(nbd)Cl]_2$ were estimated to be $(13.1 \pm 1.5) \times 10^3$ ($M_w/M_n = 2.6 \pm 0.3$) and $(63.7 \pm 4) \times 10^3$ (21.4 ± 0.4), respectively, as determined by size-exclusion chromatography using polystyrene as a standard calibrant (see the Supporting Information). The results indicate that the molecular weight distribution of the polymer prepared in the **Rh(nbd)·apo-Fr** cage is narrower than that obtained using $[Rh(nbd)Cl]_2$ in the absence of apo-Fr. On the basis of the molecular

extinction coefficient of polyphenylacetylene at 383 nm,[34,39] 235 ± 35 phenylacetylene monomers per each apo-Fr molecule were converted to polyphenylacetylene. The M_n of the polyphenylacetylene produced by **Rh(nbd)·apo-Fr** ($13.1 \pm 1.5 \times 10^3$) indicates that the polymer is composed of 130 monomers. Thus, it is expected that two polymer chains are formed within the discrete space of apo-Fr. When 6000 equiv. of phenylacetylene monomers (3.0 mM) were reacted with **Rh(nbd)·apo-Fr** (0.5 μM) for 3, 6, 9, and 12 h, 320 ± 36, 541 ± 72, 729 ± 40, and 811 ± 95 monomers are polymerized with M_n (9.4×10^3, 9.3×10^3, 8.3×10^3, and 10.0×10^3) and M_w/M_n (2.4, 2.5, 2.1, and 2.4), respectively. The number of phenylacetylene monomers at 12 h (811 ± 95 monomers, 5.0 M) is comparable to almost half concentration of neat phenylacetylene (1479 monomers, 9.1 M) in the apo-Fr cage. The value is thought to be the saturated concentration in the apo-Fr because the number is almost maintained even after 18 h (841 ± 101). The results suggest that approximately eight polymer chains are formed in the cage. Thus, the most of rhodium complexes in **Rh(nbd)·apo-Fr** can not serve as the catalysts of the polymerization. Surprisingly, the molecular weight of the resulting polymer is independent of the reaction time and the monomer concentration within the cage. The regulation of the polymerization appears to be influenced by the size and environment of the interior space of apo-Fr. Further investigations are in progress to completely elucidate the mechanism.

In order to examine the scope of **Rh(nbd)·apo-Fr** reactivity, derivatives of phenylacetylene bearing carboxylic acid, phosphonic acid, or amino groups were employed. The UV−vis spectral changes in the polymerization of phenylacetylene derivatives showed that monomers bearing carboxylic or phosphonic acid substitutents were not polymerized by **Rh(nbd)·apo-Fr**, although a monomer with an amino group was polymerized under these conditions. In the absence of apo-Fr, all of the phenylacetylene derivatives are polymerized by $[Rh(nbd)Cl]_2$ under these conditions (see the Supporting Information). These results indicate that anionic monomers encounter difficulties in penetrating into the **Rh(nbd)·apo-Fr** cage because of repulsion between the negative charges of the monomer and the anionic interior surface of the 3-fold axis channel, which consists of three aspartic acids and three glutamic acids (Figure 1c).[14]

In summary, we have demonstrated that Rh(nbd) complexes immobilized within the discrete space of apo-Fr can catalyze the polymerization of phenylacetylene with restricted molecular weight and a narrow molecular weight distribution in aqueous solution. Moreover, just a few polymer chains are prepared within the apo-Fr cage. The cage could be useful for investigating the behavior of a single polymer chain isolated in a nano-sized space.

Acknowledgment. We thank the members of BL41XU of SPring-8 for assistance during the diffraction data collection. This work was supported by a grant from the Global COE Program in Chemistry, Nagoya University (to S.A.), a Grant-in-Aid for Scientific Research (Grant 18685019 to T.U.), and Priority Areas (Grant 16033226, Chemistry of Coordination Space, to Y.W.) from the Ministry of Education, Culture, Sports, Science and Technology, Japan, and PRESTO, JST. Support from the Association for the Progress of New Chemistry and the Ogasawara Foundation for the Promotion of Science and Engineering is also acknowledged. The synchrotron radiation experiment was conducted under the approval of 2006A1782 at SPring-8.

Supporting Information Available: Experimental details and X-ray crystallographic data. This material is available free of charge via the Internet at http://pubs.acs.org.

References

(1) Vriezema, D. M.; Aragonès, M. C.; Elemans, J. A. A. W.; Cornelissen, J. J. L. M.; Rowan, A. E.; Nolte, R. J. M. *Chem. Rev.* **2005**, *105*, 1445–1490.
(2) Meldrum, F. C.; Wade, V. J.; Nimmo, D. L.; Heywood, B. R.; Mann, S. *Nature* **1991**, *349*, 684–687.
(3) Uchida, M.; Klem, M. T.; Allen, M.; Suci, P.; Flenniken, M.; Gillitzer, E.; Varpness, Z.; Liepold, L. O.; Young, M.; Douglas, T. *Adv. Mater.* **2007**, *19*, 1025–1042.
(4) Comellas-Aragonès, M.; Engelkamp, H.; Claessen, V. I.; Sommerdijk, N. A. J. M.; Rowan, A. E.; Christianen, P. C. M.; Maan, J. C.; Verduin, B. J. M.; Cornelissen, J. J. L. M.; Nolte, R. J. M. *Nat. Nanotechnol.* **2007**, *2*, 635–639.
(5) Ueno, T.; Abe, S.; Yokoi, N.; Watanabe, Y. *Coord. Chem. Rev.* **2007**, *251*, 2717.
(6) Wang, Q.; Lin, T. W.; Tang, L.; Johnson, J. E.; Finn, M. G. *Angew. Chem., Int. Ed.* **2002**, *41*, 459–462.
(7) Hooker, J. M.; Kovacs, E. W.; Francis, M. B. *J. Am. Chem. Soc.* **2004**, *126*, 3718–3719.
(8) Vriezema, D. M.; Hoogboom, J.; Velonia, K.; Takazawa, K.; Christianen, P. C. M.; Maan, J. C.; Rowan, A. E.; Nolte, R. J. M. *Angew. Chem., Int. Ed.* **2003**, *42*, 772–776.
(9) Crooks, R. M.; Zhao, M. Q.; Sun, L.; Chechik, V.; Yeung, L. K. *Acc. Chem. Res.* **2001**, *34*, 181–190.
(10) Sato, S.; Iida, J.; Suzuki, K.; Kawano, M.; Ozeki, T.; Fujita, M. *Science* **2006**, *313*, 1273–1276.
(11) Murase, T.; Sato, S.; Fujita, M. *Angew. Chem., Int. Ed.* **2007**, *46*, 1083–1085.
(12) Rebek, J. *Angew. Chem., Int. Ed.* **2005**, *44*, 2068–2078.
(13) Varpness, Z.; Peters, J. W.; Young, M.; Douglas, T. *Nano Lett.* **2005**, *5*, 2306–2309.
(14) Ueno, T.; Suzuki, M.; Goto, T.; Matsumoto, T.; Nagayama, K.; Watanabe, Y. *Angew. Chem., Int. Ed.* **2004**, *43*, 2527–2530.
(15) Douglas, T.; Young, M. *Nature* **1998**, *393*, 152–155.
(16) Liu, X. F.; Theil, E. C. *Acc. Chem. Res.* **2005**, *38*, 167–175.
(17) Harrison, P. M.; Arosio, P. *Biochim. Biophys. Acta* **1996**, *1275*, 161–203.
(18) Yang, X. K.; Chasteen, N. D. *Biophys. J.* **1996**, *71*, 1587–1595.
(19) Douglas, T.; Dickson, D. P. E.; Betteridge, S.; Charnock, J.; Garner, C. D.; Mann, S. *Science* **1995**, *269*, 54–57.
(20) Kramer, R. M.; Li, C.; Carter, D. C.; Stone, M. O.; Naik, R. R. *J. Am. Chem. Soc.* **2004**, *126*, 13282–13286.
(21) Klem, M. T.; Resnick, D. A.; Gilmore, K.; Young, M.; Idzerda, Y. U.; Douglas, T. *J. Am. Chem. Soc.* **2007**, *129*, 197–201.
(22) Iwahori, K.; Yoshizawa, K.; Muraoka, M.; Yamashita, I. *Inorg. Chem.* **2005**, *44*, 6393–6400.
(23) Ueno, T.; Abe, M.; Hirata, K.; Abe, S.; Suzuki, M.; Shimizu, N.; Yamamoto, M.; Takata, M.; Watanabe, Y. *J. Am. Chem. Soc.* **2009**, *131*, 5094–5100.
(24) Niemeyer, J.; Abe, S.; Hikage, T.; Ueno, T.; Erker, G.; Watanabe, Y. *Chem. Commun.* **2008**, 6519–6521.
(25) Abe, S.; Niemeyer, J.; Abe, M.; Takezawa, Y.; Ueno, T.; Hikage, T.; Erker, G.; Watanabe, Y. *J. Am. Chem. Soc.* **2008**, *130*, 10512–10514.
(26) Tang, B. Z.; Poon, W. H.; Leung, S. M.; Leung, W. H.; Peng, H. *Macromolecules* **1997**, *30*, 2209–2212.
(27) Maeda, K.; Goto, H.; Yashima, E. *Macromolecules* **2001**, *34*, 1160–1164.
(28) Richens, D. T. *The Chemistry of Aqua Ions*; Wiley: Chichester, U.K., 1997; pp 439−490.
(29) Koelle, U. *Coord. Chem. Rev.* **1994**, *135*, 623–650.
(30) Hempstead, P. D.; Yewdall, S. J.; Fernie, A. R.; Lawson, D. M.; Artymiuk, P. J.; Rice, D. W.; Ford, G. C.; Harrison, P. M. *J. Mol. Biol.* **1997**, *268*, 424–448.
(31) Granier, T.; Comberton, G.; Gallois, B.; d'Estaintot, B. L.; Dautant, A.; Crichton, R. R.; Precigoux, G. *Proteins* **1998**, *31*, 477–485.
(32) Atomic coordinates for **Rh(nbd)·apo-Fr** are deposited in the Protein Data Bank as entry 2ZUR.
(33) Datta, S.; Mori, Y.; Takagi, K.; Kawaguchi, K.; Chen, Z. W.; Okajima, T.; Kuroda, S.; Ikeda, T.; Kano, K.; Tanizawa, K.; Mathews, F. S. *Proc. Natl. Acad. Sci. U.S.A.* **2001**, *98*, 14268–14273.
(34) Cametti, C.; Codastefano, P.; D'Amato, R.; Furlani, A.; Russo, M. V. *Synth. Met.* **2000**, *114*, 173–179.
(35) Webb, B.; Frame, J.; Zhao, Z.; Lee, M. L.; Watt, G. D. *Arch. Biochem. Biophys.* **1994**, *309*, 178–183.
(36) Simionescu, C. I.; Percec, V. *J. Polym. Sci., Part A: Polym. Chem.* **1980**, *18*, 147–155.
(37) Kanki, K.; Nakazato, A.; Nomura, R.; Sanda, F.; Masuda, T. *J. Polym. Sci., Part A: Polym. Chem.* **2004**, *42*, 2100–2105.
(38) Claverie, J. P.; Soula, R. *Prog. Polym. Sci.* **2003**, *28*, 619–662.
(39) The molecular extinction coefficient of polyphenylacetylene (3.16×10^3) was measured in $CHCl_3$.

JA901234J